Radiation Measurements 44 (2009) 724–728

Contents lists available at ScienceDirect

Radiation Measurements

journal homepage: www.elsevier.com/locate/radmeas

Fluence and dose of mixed space radiation by SSNTDs achievements and constraints

J.K. Pálfalvi*

HAS KFKI, Atomic Energy Research Institute, P.O. Box 49, H-1525 Budapest, Hungary

ARTICLE INFO

Article history:
Received 22 October 2008
Accepted 17 October 2009

Keywords:
Space dosimetry
SSNTD
Proton detection

ABSTRACT

The space radiation can be characterized in several ways: considering its origin, particle type and energy or by registration technique. From the point of view of solid state nuclear track detectors (SSNTD) applied for space dosimetry one way of characterization is to distinguish external radiation (primary cosmic ray particles and projectile fragments entering the detector from the surroundings) and internal radiation (secondary particles like target fragments and recoiled ions which are formed mostly by protons and neutrons inside the detector material). The measurable quantities are always the track parameters on the etched surface of the detector sheet, which must be enough to derive the particle fluence, based on reasonable theoretical approach. The "classical" or "conventional" method to obtain the fluence and dose does not distinguish between tracks induced by external or internal particles, and this may introduce systematical errors and generate higher uncertainty, and over- or underestimation of the dose. The latter consequence is demonstrated after the brief description of the classical method. Since the most abundant particles in space are protons, the study deals –as an example- with the determination of the high energy proton induced secondary particle forming events inside the detector, based on experiments.

1. Introduction

To provide appropriate shelter for astronauts, the knowledge of the composition of the space radiation outside and inside of a space vehicle is mandatory. Particles which can be detected by a specific SSNTD may range from the Earth magnetic field trapped protons to the high atomic number and energy (HZE) particles. The most important from the point of view of the absorbed dose can be the detection of protons since they are the most abundant particles in the space radiation field. The high energy protons can be detected only via their secondaries produced by spallation process of the constituent elements of the detector material. Usually the space radiation field on the place of measurements can be considered to be isotropic and homogeneous. However, only dose particles can be detected by the SSNTDs which pass certain requirements: their linear energy transfer (LET) should be higher than a material dependent threshold (L_t) and their incident angel in respect to the detector surface is above a critical value (Θ_c). To determine the incident particle fluence, it requires investigation of individual tracks of particles induced in the detector and revealed by chemical etching. The track parameters measured by an appropriate image analyzer are generally the major and minor axes (a, b) of the track opening on the surface of the detector sheet. Several assumptions about the particle energy deposition mechanism are then necessary to obtain from these geometrical parameters useful physical quantities as the track etch velocity (V_T) which is needed to calculate the fluence as shown later. The track development kinetics has been described by many authors (Somogyi and Szalay, 1973; Durrani and Bull, 1987; Nikezic, 2000, 2003) who did emphasize the consequences of application of physically not always realistic assumptions. Since V_T is the basic quantity in track detection a special attention is to be paid on how to determine and use it. A track can be developed only if $V_T > V_B$, where the latter one is the bulk etch rate of the detector material

2. Determination of fluence

2.1. Classical method

According to the "classical method" it is assumed that the V_T is constant along the particle path inside the detector material. If we accept this then the track and bulk etch rate ratio, $V = V_T/V_B$, can be calculated by the following formula (Durrani and Bull, 1987):

* Tel.: +36 1 392 2222 1495; fax: +36 1 395 9162.
E-mail address: palfalvi@aeki.kfki.hu

1350-4487/$ – see front matter © 2009 Elsevier Ltd. All rights reserved.
doi:10.1016/j.radmeas.2009.10.045

$$V = \frac{\sqrt{\left(1-B^2\right)^2+4A^2}}{1-B^2}, \quad (1)$$

where A=$a/2h$ and B=b/2h (a is the measured major-, b is the minor axis, h is the etched off layer thickness, $h = V_B t$, t is the etching time). For the critical angle then the following formula is valid:

$$\cos^2\Theta_c = \frac{V^2-1}{V^2} \quad (2)$$

If the differential fluence at a given point x is defined by the next formula:

$$\Phi(\Omega,x) = \frac{d^2N}{dAd\Omega}, \quad (3)$$

then considering the relation between the critical and the detection angles as shown in Fig. 1 the fluence can be deduced (in detail in Benton, 2004)

$$\Phi(\Omega,x) = \left(A2\pi\cos^2\Theta_c\right)^{-1}N, \quad (4)$$

here A is the area of detector where the detected particle number is N.

The V is a LET dependent quantity. If the relationship between them is known, then the LET can be calculated and the fluence can be expressed also by LET. In practice, the fluence is binned into equal LET intervals in order to calculate the absorbed dose. The binned fluence vs. LET is called differential LET spectrum $\Phi_i(\Omega,L,x)$ or $\boldsymbol{\Phi_i}$.

It is done in the following way:

1. From the measured track parameters (usually minor and major axes) calculate the $\boldsymbol{V}$ for each particle (all together $\boldsymbol{N}$) counted on an area of $\boldsymbol{A}$.
2. Convert the $\boldsymbol{V}$ to $\boldsymbol{L}$ (LET) for each particle applying a calibration function (this is further discussed in 2.2).
3. Select an appropriate LET interval (for instance 5 keV/μm) $\boldsymbol{dL}$.
4. Sort the particles according to their LET into $\boldsymbol{dL_i}$ resulting in the differential track number $\boldsymbol{N_i}$, $\boldsymbol{i}$ runs from the lowest detectable LET interval, logically, up to the last LET interval covered by calibration.
5. Calculate the average $\boldsymbol{V_i}$ for each $\boldsymbol{dL}_i$.
6. Calculate the average $\boldsymbol{\cos^2\Theta_{c,i}}$ for each $\boldsymbol{dL}_i$, see Equation (2).
7. Calculate the $\boldsymbol{\Phi_i}$ for each $\boldsymbol{dL}_i$ using Equations (4) and divide it by the length of the interval. This will be a "step function".
8. Apply corrections taking into consideration some facts influencing the particle detection ability of the detector (this is further discussed later).

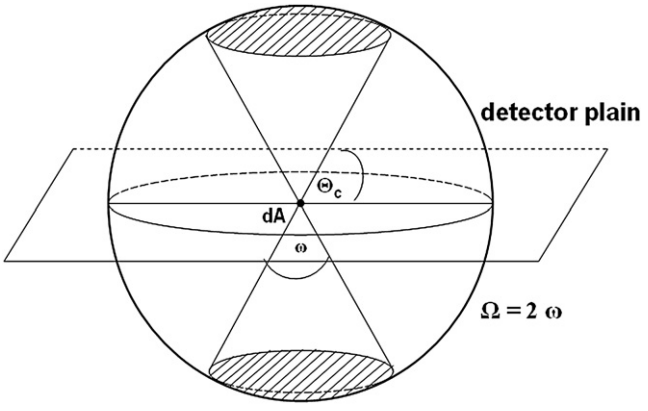

Fig. 1. Assuming isotropic radiation filed the detection solid angle (Ω) is determined by the critical angle (Θ_c). Those particles crossing the shaded spherical area and incident on detector area dA will be detected.

2.2. Calibration

During the calibration a relationships is constructed between the quantity V "measured" after a given layer removal (h, see Equation (1)) by etching and the particle LET when passing through the original surface of the detector. For the purpose detectors are exposed to radiation with known LET and perpendicular incidence and etched. If V is constant as supposed by the "classical method" then the relationship is independent from the h until the track is not over etched. However, for space radiation it is not always true as seen in Figs. 2 and 3.

It is seen that the calibration curves obtained by 6 and 15 h etching differ from each other above ~150 keV/μm, which indicates that the constant V assumtion cannot be accepted here.

It is usual that the varying V_T is expressed vs. the residual range ($R' = R - l - h/\sin\varphi$, R is the particle range, l is the track length and φ is the incident angle) and given by some well-behaving analytical function (Nikezic, 2000). Then applying appropriate mathematical procedure the track parameters (axes a, b) can be calculated for a given etching time. In a theoretical experiment the track exes of alpha particles ($E_\alpha = 4.5$ MeV, incident at different angles) were calculated by the computer code developed by Nikezic, 2003. The validity of the utilized V_T function has been proved experimentally. Then from the axes obtained the V values were re-calculated using Equation (1). The results are presented in Fig. 4.

It is evident that the V (and LET) of a particle should not depend on the incident angle in the same detector material. The curve related to 6 h etching shown in Fig. 4 indicates an incident angle dependence which means that accepting the constant V_T assumtion by applying Equation (1) false V results can be obtained from realistic track axes data, which further results in false LET if the calibration function presented in Fig. 3 is applied. It is to be mentioned that the critical angle for 4.5 MeV alpha particle is around 20 °, which means that the curve below 25 ° is not realistic even for 6 h etching time.

The V dependence on etching time as seen in Fig. 4 rises another question: how to calculate the V if the tracks are long etched, in other words: over etched?

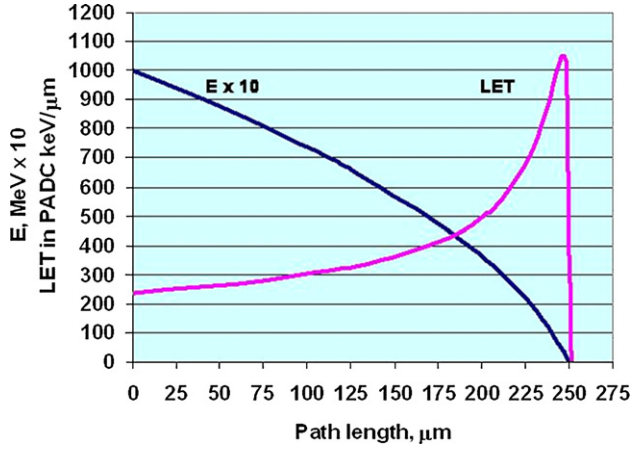

Fig. 2. Energy and LET of 100 MeV Carbon ion along the particle path in poliallyldiglycol-carbonate (PADC) SSNTD calculated by SRIM2003 code. The LET is steaply increasing along the particle path, consequently also the V.

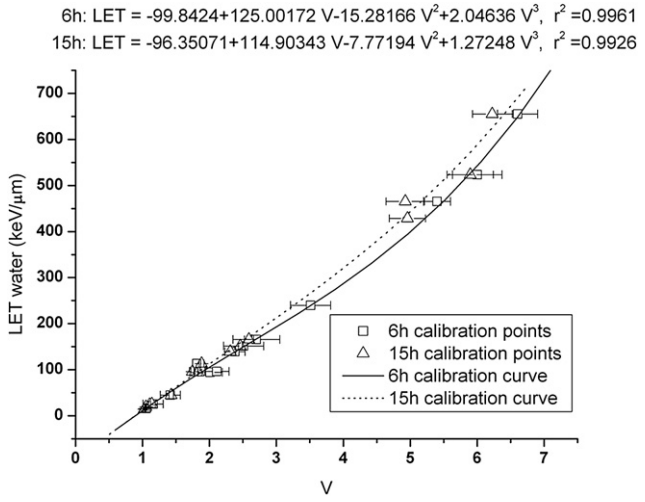

Fig. 3. Calibration functions obtained by exposing the detectors to different ions and etched for 6 and 15 h, removing 8 and 20.1 μm bulk layers, respectively.

To answer the question needs further studies. Up to now two methods are in use to treat the over etched tracks: to consider them as normal tracks, this leads to the over estimation of V and the LET and consequently also the dose, which is anyhow a conservative way. Someone may neglect these tracks, if it is possible to separate them from normal tracks by measurements. The consequence is the underestimation of the dose.

2.3. Corrections

Near the LET threshold (L_t) the detection of a particle is uncertain, the track area is small and difficult to measure it. In general, the differential LET spectrum shows a local maximum above the L_t as seen in Fig. 5.

Since the spectrum should be a monotonous one the peak indicates that the value in the first interval is under evaluated. A correction can be done applying extrapolation as shown in Fig. 5, if the L_t is considered to be 10 keV/μm. Different detector materials may need different correction methods as described by Doke et al., 1997.

Corrections should be done also when the sensitivity of the detector is supposed to be altered due to track fading (Zhou et al., 2007) or extreme flight conditions like decreased atmospheric pressure and oxygen content, etc. or simple by using a batch of production other than used for calibration. It is recommended to expose the detectors before and during the flight exposure to preferably an alpha source with known LET in order to control the shifting of the LET spectrum. Also the so called in-flight self-calibration is widely used when the detection of peaks in the LET spectrum (L_∞ in water) of stopping protons (at 84 keV/μm) and relativistic irons (at 135 keV/μm) are used to make correction (Zhou et al., 2007).

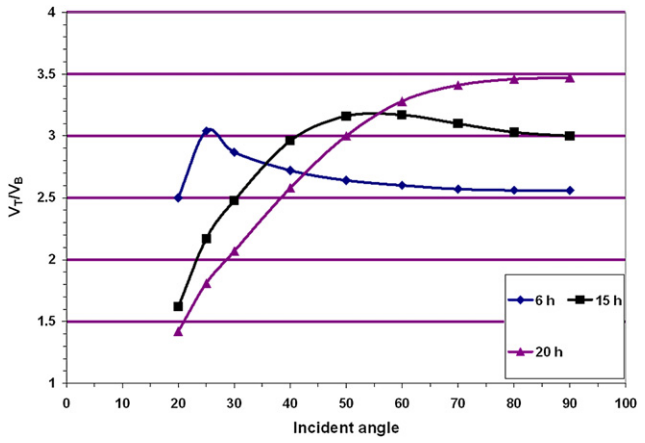

Fig. 4. The false variation of the track etch rate ratio vs. the incident angle of an alpha particle of 4.5 MeV. The parameter is the etching time. 6 h etching fully develops the track up to the end of the particle range. Prolonged etching causes over etched track. More explanation in the text.

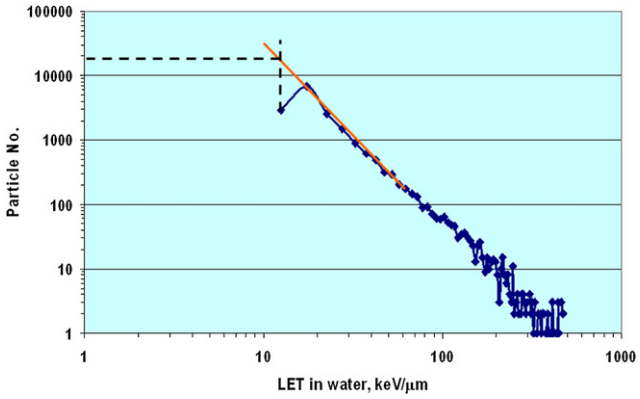

Fig. 5. LET spectrum obtained inside the Service Module of the International Space Station in 2007. The points are shown in the middle of the 5 keV/μm intervals. The detector was etched for 15 h, removing 20.1 μm layer.

In all cases, validation of the applied corrections and uncertainty analysis are necessary to ensure that the accuracy requirements are met (NCRP, 2002).

3. Dose assessment

To estimate the delayed stochastic effect of space radiation the determination effective dose is necessary for what the basic quantity is the mean absorbed dose in an organ or tissue as recommended the NCRP, 2001, 2002. It is calculated from the distribution of the absorbed dose (D) at points in the organ or tissue in terms of the LET contributions at the specific points and averaged over the organ or tissue. The absorbed dose in water ($\rho = 1$ g/cm^3) and the dose equivalent are given by the equations (6) and (7). The fluence is given in cm^{-2} sr^{-1} keV^{-1} μm. The point dose is calculated from the LET using the formula:

$$\frac{\delta E}{\delta x} = L(x) \rightarrow L_i, \tag{5}$$

Assuming isotropic radiation field the integration is done over 4π.

$$D = 4\pi \times 1.6 \times 10^{-6} \times \frac{1}{\rho} \times \Sigma\left(\Phi_i(L) \times \bar{L}_i \times dL_i\right), \tag{6}$$

$$H = 4\pi \times 1.6 \times 10^{-6} \times \frac{1}{\rho} \Sigma\left(\Phi_i(L) \times \bar{L}_i \times Q_i(L) \times dL_i\right), \tag{7}$$

The $Q_i(L)$ is the LET dependent quality factor, $\bar{L}_i$ is the mean LET (linear collision stopping power for L_∞) in the given dL_i interval (both in keV/μm), the constant 1.6×10^{-6} is applied to harmonize the units to obtain the D and H in mGy and mSv, respectively. Then the averaged quality factor is the ratio of H and D,

$$Q = H/D. \tag{8}$$

In the case of directional dependence of the fluence the dose should be calculated separately for the different solid angles and summed up.

The uncertainty of the dose determination is highly dependent on the knowledge of the fluence. It is emphasized again that the "classical" or conventional method assumes the constant V, which may be valid for the long range particles, when the LET changes very slowly along the particle path. This is not valid, however, for the secondary particles like target fragments induced by high energy protons and neutrons or induced by nuclear reactions as it is shown in the next paragraph.

4. Proton induced target fragmentation

The purpose of the investigations was to estimate the real number and LET of secondary particles (fragments) produced by high energy (>50 MeV) trapped and GCR protons in a close tissue equivalent solid state nuclear track detector material. The PADC material is composed of $C_{12}H_{18}O_7$, which indicates that ($p \rightarrow {}^{12}C$) is the most important fragmentation interaction, however, in practice the ^{16}O fragmentation also may play a considerable role. In this study we present some results obtained from the p → ^{12}C interaction investigations. The detector contains two adjacent layers of PADC material.

Target fragments from C are p, D, ^3He, α, Li, Be B and C, mostly two particles from one interaction. Particles with $Z > 2$ have energy and range well below 10 MeV and 10 μm, resp. with a peak around 2–3 MeV, The energy of α particles may extend beyond 10 MeV, up to ~20 MeV. Secondary protons may have high energy, close to the projectile proton energy and escape from the active volume without a second interaction or significant energy deposition. Etchable tracks will be produced by the heavier particles, $Z > 1$.

Based on the track formation mechanism illustrated in Fig. 6 one could proceed (following the formulation given in Durrani and Bull, 1987, pp. 64–69):

if $\boldsymbol{n}$ is the fragmentation event producing two fragments in a unit volume then the number of tracks detected on unit detector surface (called track density, $\boldsymbol{T}$) can be expressed as

$$T = T_1 + T_2 = \frac{1}{2} n \times \left(R_1 \sin^2 \Phi_c + R_2 \sin^2 \Theta_c\right), \quad (9)$$

where T_1 and T_2 are the track densities of the two different types of fragments (^3He and ^{10}B, for instance) having ranges R_1 and R_2, with critical detection angles Φ_c and Θ_c, respectively. The number of the tracks of detected pairs is

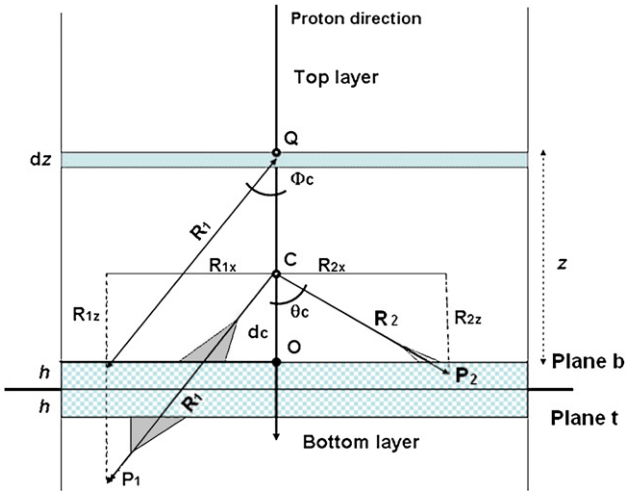

Fig. 6. Track formation geometry showing the incident proton and two forward moving fragments induced in point C. Both particles are detected by the upper detector. If point C moves upward then only one particle or above point Q none can be detected.

$$2T_2 = n \times R_2 \sin^2 \Theta_c \quad (10)$$

and number of the lost particles is then

$$N_L = T - 2T_2 = \frac{1}{2} n \times \left(R_1 \sin^2 \Phi_c - R_2 \sin^2 \Theta_c\right) \quad (11)$$

Let us define the efficiency ε as the ratio of the measured track density over the generated particle number ($\boldsymbol{2n}$) in a unit volume then we receive:

$$\varepsilon = \frac{T}{2n} = \frac{1}{4}\left(R_1 \sin^2 \Phi_c + R_2 \sin^2 \Theta_c\right) \quad (12)$$

Model calculations and experiments may help to obtain the ranges and critical angles to be considered in an actual case. For instance, if $\boldsymbol{R_2} = 10$ μm is the averaged ranged of heavy products and $\boldsymbol{R_1} = 300$ μm is the averaged range of light particles, as well as, averaged Φ_c and Θ_c, are 70° and 45°, respectively, then $\varepsilon = 6.8 \times 10^{-3}$ cm.

When the detector stack was exposed perpendicularly to 170 MeV protons (simulating trapped protons) with a fluence of 5.5×10^8 cm^{-2} the measured track density on the bottom side (1b) of the first detector sheet was found to be $T = 3.8 \times 10^4$ cm^{-2}. (See LET spectra in Fig. 7). Then, the number of particles in unit volume (1 cm^3) is $2n = T/\varepsilon$, numerically, applying the above calculated $\boldsymbol{\varepsilon}$, $2n = 5.6 \times 10^6$ vs. $\boldsymbol{T}$! Only ~0.7% is detected. However, all the $\boldsymbol{2n}$ particles having short range would contribute to the absorbed dose within the unit volume. This special case can easily be generalized assuming isotropic proton field and realistic proton spectrum (the fragment production cross-section is nearly constant above 100 MeV). However, the detection efficiency, ε, would remain close to that one shown above (Palfalvi et al., submitted for publication).

In an idealized case the primary, long range particles can be separated from the target fragments, then the dose from latter ones can be separately estimated and added to the dose of long range particles applying a correction based on the knowledge of the detection efficiency. This method may improve the dose assessment and would increase the accuracy of the dose determination. The contribution of the target fragments to the total dose depends on the proton contribution to the space radiation field.

Investigating Fig. 7 it can be concluding that the target fragment LET spectrum is less steep than that one obtained on the ISS below

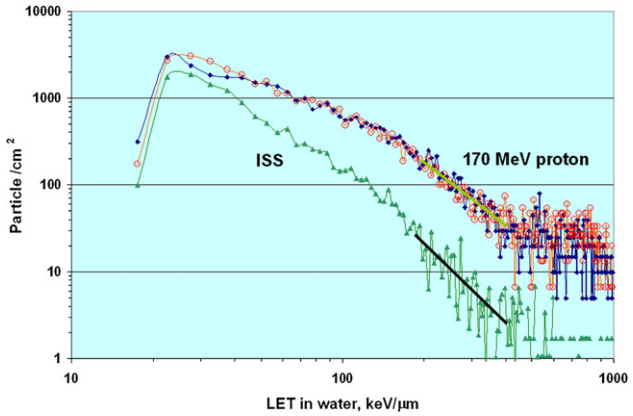

Fig. 7. 170 MeV proton induced LET spectra on the adjacent surfaces of the detector stack and spectrum on the ISS after 6 h etching (8 μm bulk layer removal, no over etched tracks).

$\sim$150 keV/μm, indicating that the primary particles are dominant here. Above it the slopes are very close, suggesting that the detected particles are mostly fragments in both cases. Considering the high quality factor of fragments, their role seems to be important, therefore, if we are aware of the ratio of the detected and lost particles then the correction should be done to eliminate the underestimation of the dose.

5. Summary

It was pointed out that the "classical" or "conventional" determination of the primary cosmic ray fluence and the dose suffers of several problems:

- neglecting the variation of the V along the particle path by applying Equation (1). results in an overestimation of the V and consequently of the LET and finally of the dose.
- The result is the same if the over etched tracks (internal tracks) are not separated and the Equation (1) is applied to calculate their V.
- From high energy proton exposures it became clear that the majority of high LET tracks, which may be over etched if long etching time is applied, are due to target fragmentation (internal tracks). Their detection efficiency can be determined and a correction can be applied to improve the accuracy of the dose determination.
- The classical method says: if an incident particle cannot produce a track then that particle should not be considered at all. This can be accepted for low LET particles ($<$10 keV/μm), their dose contribution can be measured by other methods (TLD). However, target fragments where $Z > 2$ may have short range which hampers their detection but they are present being very close to their pair particle which is detected, therefore, they contribute to the dose in a very small volume (point dose) should not be neglected.

Finally, the "classical" method is presently an accepted way of dose assessment and widely used, however, this should not prevent the further development based on new information and more sophisticated technical support.

Acknowledgments

The author is tanking the staff of the Svedberg Laboratory at University of Uppsala, Sweden for the high energy proton exposure. The support of the Hungarian Space Office (TP-174) in the ISS experiments is highly acknowledged.

References

Benton, E.R. 2004. Radiation Dosimetry at Aviation Altitudes and in Low-Earth Orbit, Ph.D. thesis, University College, Dublin, Ireland.
Doke, T., Hajashi, T., Kobayashi, M., Watanabe, A., 1997. Dip angle dependence on track formation sensitivity in antioxidant doped CR-39 plates. Rad. Meas. 18, 445–450.
Durrani, S.A., Bull, R.K., 1987. Solid State Nuclear Track Detection: Principles, Methods, and Applications. Pergamon Press, Oxford, p. 284.
NCRP Report No. 137 2001. Fluence-based and Microdosimetric Event-based Methods for Radiation Protection in Space.
NCRP Report No. 142 2002. Operational Radiation Safety Program for Astronauts in Low Earth Orbit: A Basic Framework.
Nikezic, D., 2000. Three-dimensional analytical determination of track parameters. Rad. Meas. 32, 277–282.
Nikezic, D., 2003. Three-dimensional analytical determination of track parameters: over-etched tracks. Rad. Meas. 37, 39–45.
Pálfalvi, J. K., Szabó J., Eördögh, I. Detection of high energy neutrons, protons and He particles by Solid State Nuclear Track Detectors. Submitted to Rad. Meas. submitted for publication.
Somogyi, G., Szalay, S.A., 1973. Track-diameter kinetics in dielectric track detectors. Nucl. Inst. Meth. 109, 211–232.
Zhou, D., Semones, E., Gaza, R., Johnson, S., Zapp, N., Weyland, M., 2007. Radiation measures for ISS-Expedition12 with different dosimeters. Nucl. Inst. Meth. A 580, 1283–1289.